ORIGINAL ARTICLE

Tool condition monitoring in milling process using multifractal detrended fluctuation analysis and support vector machine

Jingchao Guo [1,2] · Anhai Li [1,2] · Rufeng Zhang [1,2]

© Springer-Verlag London Ltd., part of Springer Nature 2020

Abstract

Tool wear will lead to the reduction of surface quality and machining accuracy. Therefore, tool condition monitoring is vital to the improvement of industrial production efficiency and quality. In this paper, first of all, the internal mechanism of the milling process and the performance characteristics of the milling signals were analyzed. It is found that there are different trends between the large and small fluctuations of milling signals in the process of tool wear increasing. This property can be characterized by various parameters of multifractal spectrum to establish the relationship between tool wear and multifractal parameters. By analyzing the changes of multifractal spectrum parameters, the tool wear monitoring can be realized. Then, the multifractal detrended fluctuation analysis (MFDFA) method is used to calculate the mean square error, generalized Hurst exponent, and multifractal spectrum parameters, which are the eigenvectors, and establish its relationship with tool wear. Finally, the tool condition diagnosis is conducted by a support vector machine (SVM). The results show that the tool condition monitoring method of MFDFA combined with SVM is proved to be effective and the multifractal parameters of MFDFA are very sensitive to tool wear.

Keywords Tool condition monitor · Cutting force signal · Vibration signal · Multifractal detrended fluctuation analysis · Support vector machine

1 Introduction

Tool wear is the result of mechanical friction, cutting force, and cutting temperature in milling process. It is a very complex phenomenon of physical and chemical changes, which consists of abrasion, adhesion, diffusion, fatigue, and chemical wear [1]. In the process of cutting, the tool contacts with the workpiece directly. The tool wear will increase the roughness of the workpiece surface and reduce the quality of the workpiece. Serious tool wear will cause tool chipping, fracture, and chatter, which will damage the workpiece and machine tool and cause serious processing accidents [2]. Therefore, in order to obtain better surface quality and reduce

the loss caused by tool wear, the research of signal processing and pattern recognition technology for tool condition monitoring has become an urgent problem to be solved [3].

Tool condition monitoring can be divided into direct methods and indirect methods based on the method of measurement technique and complexity of the machining process [4]. The direct methods based on direct measurement of flank wear consist of vision inspection [5], radioactivity [6], and electrical resistance [7]. However, because of the high requirements for the measuring environment and the limitations of accessing such as cutting fluid, illumination, and chip, the direct methods are not conducive to practical applications [8]. The indirect methods refer to measure tool wear based on the signal analysis. By the signals obtained from the cutting process, such as cutting force [9, 10], vibration [11, 12], acoustic emission [13, 14], temperature [15], and motor current [16], the hidden relationship between these signals and tool wear is analyzed to indirectly measure tool wear. Among these sensors, cutting force, vibration, and acoustic emission have been used more frequently than other sensors. Cutting force is an intuitive reflection of the changes of various factors in the cutting process, which is closely related to the cutting

✉ Anhai Li
anhaili@sdu.edu.cn

1 Key Laboratory of High Efficiency and Clean Mechanical Manufacture of MOE, School of Mechanical Engineering, Shandong University, Jinan 250061, China

2 National Demonstration Center for Experimental Mechanical Engineering Education, Shandong University, Jinan 250061, China

process, so the cutting force signal is effective. Vibration signal monitoring equipment is inexpensive and easy to install. Acoustic emission signal, mainly caused by plastic deformation of workpiece and chip, friction between tool and workpiece, and chip fracture, whose frequency range is between 10 kHz and 10 MHz, has a higher frequency than mechanical vibration and environmental noise. So it has the advantages of high sensitivity and strong anti-interference ability.

Feature extraction is a key step after signal processing. On the one hand, feature extraction can remove irrelevant redundant information and select features related to tool wear as input of the model. On the other hand, the purpose of feature extraction is to control the number of selected features and select the most relevant features, which can reduce the computing time of feature extraction and model construction. There are a lot of feature extraction methods; for instance, time domain and frequency domain analysis [17, 18], wavelet transform (WT) [19, 20], and empirical mode decomposition (EMD) [21]. Time domain and frequency domain analyses are commonly used feature extraction methods, but they can only describe the characteristics of signal from a single standpoint and cannot provide comprehensive feature information. They have limitations in dealing with non-stationary signals [22]. WT and EMD can remedy the defect of time-frequency domain method. However, they have their own limitations. Due to the deficiency of generality in the selection of wavelet bases, it is difficult for WT to recognize new states. EMD cannot avoid mode aliasing and low computational efficiency in the face of complex signals. For this reason, some new methods applied to feature extraction have been come up, for example, fractal theory. In fractal theory, multifractal detrended fluctuation analysis (MFDFA) algorithm, which was proposed by Kantelhardt et al. [23], plays an important role in fault diagnosis. MFDFA not only pays close attention to the self-similarity but also provides the ability to describe the overall average and the local characteristics of the signal. MFDFA has been applied to the fault diagnosis of rolling bearings fault location and damage degree by Xiong et al. [24]. It has been found that the parameters of MFDFA in different states are different from each other, so it can be used to identify the fault state of rolling bearings. Liu applied MFDFA to the fault diagnosis of electromechanical actuators and successfully identified the fault states under different working conditions using the combination of variable mode decomposition (VMD) and multifractal detrended enablement analysis (MFDFA) [25].

Decision-making is also an important part in indirect methods for tool condition monitoring. Several classification methods for tool conditions have been proposed these years, for instance, artificial neural networks (ANN) [26, 27], hidden Markov model (HMM) [28, 29], support vector machine (SVM) [30, 31], and fuzzy C-means clustering [32, 33]. In this study, we choose SVM as the classification model. The

excellent performance of SVM in small sample makes it competent for TCM, which has small sample size and many nonlinear high-dimensional features. In addition, compared with ANN, SVM overcomes the problems of uncertain network structure, local minimum, over-fitting, and under-fitting in neural network algorithm. The sound signal has been collected during the end milling process by Kothuru et al. [34], and then input the SVM model to make the tool condition diagnosis decision after signal preprocessing and feature extraction by the wavelet transform. Pandiyan et al. [35] explored force, vibration, and the acoustic sensor to test the tool wear during the abrasive belt grinding process. By using the time and frequency domain features and SVM, the classification accuracy reaches up to 94.7%.

A fault diagnosis method for TCM based on MFDFA and SVM is proposed in this paper. Experiment platform is introduced in Section 2. The MFDFA technique for feature extraction and SVM for tool wear monitoring model are introduced in Section 3. Experiment result and discussion are presented in Section 4 and concluded in Section 5. The overall workflow of the tool wear monitoring process is shown in Fig. 1.

2 Experiment setup

To demonstrate the effectiveness of our contributions, we use the experimental data measured from a high-speed milling process, which is obtained from "prognostic data challenge 2010" database [36]. The experimental components are shown in Table 1, and Fig. 2 shows the experiment setup for signal acquisition.

Every cutter made 315 cuts under the same operation conditions. Seven channels of signals (cutting forces in three directions, vibration in three directions, and AE_RMS) were obtained for each cut and the LECIA MZ12.5 high-performance stereo microscope was utilized to measure the tool wear after each cut. The cutting parameters of the machining process are shown in Table 2. The whole tool life can be divided into three parts: the initial wear state, the gradual wear state, and the accelerated wear state. The initial wear state has wear value of 0~60 μm; the gradual wear state is 60~120 μm; the accelerated wear state is wear value greater than 120 μm.

3 Methods

3.1 Multifractal detrended fluctuation analysis

In recent years, the MFDFA method has been proved to be one of the most important and reliable tools in detecting the long-range correlation of non-stationary time series, and has been applied in many fields like life science, geology,
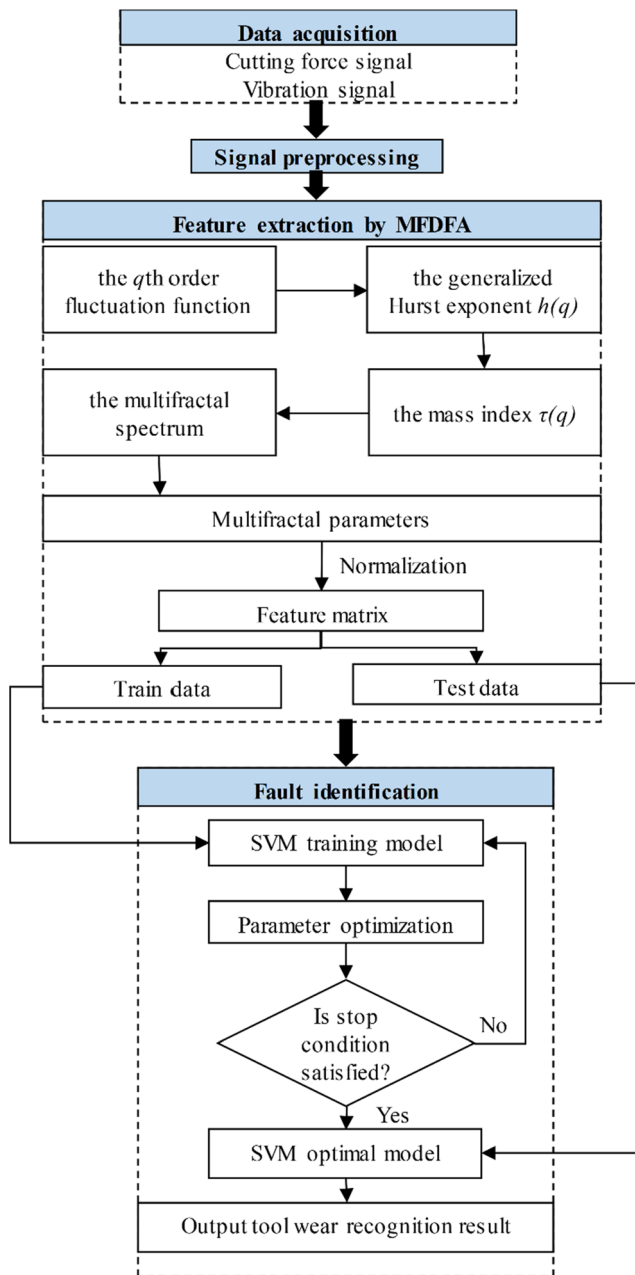
Fig. 1 Flow chart of tool condition monitoring process based on MFDFA and SVM

meteorology, and economics. From the point of view of dynamics, it is found that the transformed sequence retains the characteristics of the original sequence and maintains the

same persistence. At the same time, the transformed sequence is able to eliminate its own trend components and preserve the fluctuation components of the original sequence. The MFDFA method for non-stationary time series with length N $\{x_i, i = 1, 2, …, N\}$ can be divided into the following five steps [37]:

1. The mean value $\bar{x}$ of the time series is calculated firstly and then it should calculate the difference of the sequence between each data point x_i and the average value $\bar{x}$, determining the cumulative series:

$$y(i) = \sum_{i=1}^{n} \left(x_i - \bar{x}\right), n = 1, 2, …, N \tag{1}$$

$$\bar{x} = \sum_{i=1}^{n} x_i \tag{2}$$

2. The cumulative series $y(i)$ is partitioned into $m \equiv int\,(N/s)$ parts. Every part which is continuous and without overlapping each other has a length of s. In most cases, since N always cannot be divisible by s, it is necessary to repeat the division from the opposite end of the sequence. Consequently, $2m$ segments are obtained.

3. Fit local tendency of each part by the least-square algorithm:

$$\begin{aligned} y_v(i) = a_0 + a_1 i + a_2 i^2 + … + a_k i^k, \\ i = 1, 2, …, s; \; k = 1, 2, … \end{aligned} \tag{3}$$

where k is order polynomials and a_k are the polynomial coefficients.

4. The mean square error $F^2(v, s)$ can be calculated by the following formulas:

When $v = 1, 2, …, m$,

$$F^2(v, s) = \frac{1}{s} \sum_{i=1}^{s} \{y[(v-1)s + i] - y_v(i)\}^2 \tag{4}$$

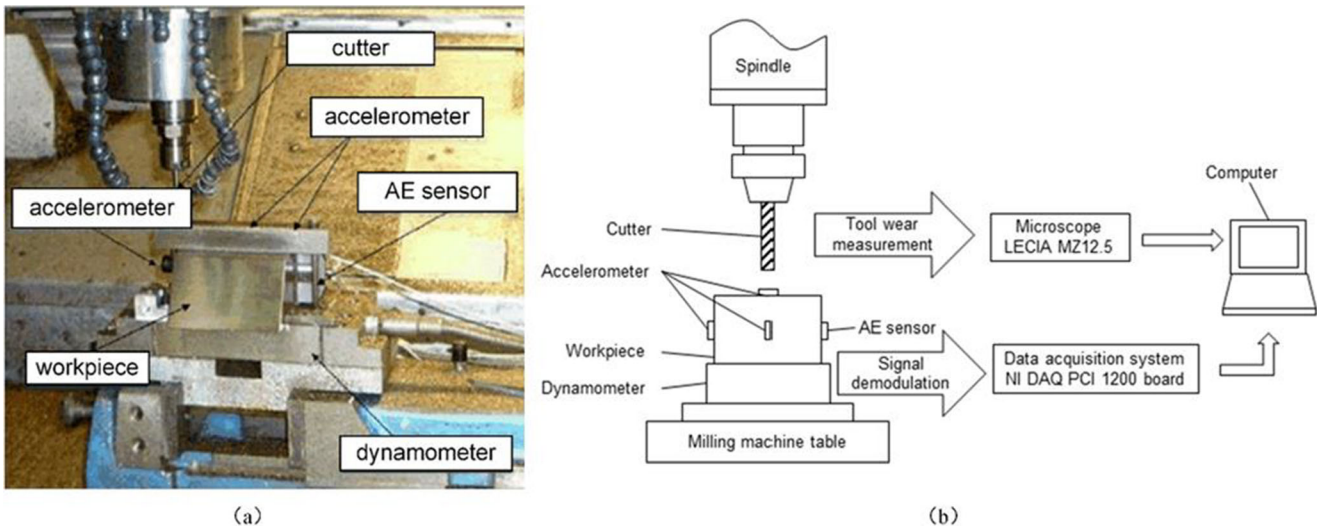| Table 1 Experimental components		
	Milling machine	Röders Tech RFM760
	Cutting tool	6-mm three-flute ball nose tungsten carbide cutter
	Workpiece	Hardened stainless steel (HRC52)
	Data acquisition system	NI DAQ PCI 1200 board
	Microscope	LECIA MZ12.5

Fig. 2 Experimental setup for tool wear monitoring. (a) Experimental setup [36]. (b) Experimental schematic diagram

When $v = m + 1, m + 2, \ldots, 2m$,

$$F^2(v, s) = \frac{1}{s} \sum_{i=1}^{s} \{y[N-(v-1)s + i]-y_v(i)\}^2 \qquad (5)$$

5. The qth order fluctuation function of $2m$ subintervals can be obtained by the following formulas:

$$F_q(s) = \left\{ \frac{1}{2m} \sum_{v=1}^{2m} \left[F^2(v, s) \right]^{q/2} \right\}^{1/q} \qquad q \neq 0$$
$$F_q(s) = \exp \left\{ \frac{1}{4m} \sum_{v=1}^{2m} \ln \left[F^2(v, s) \right] \right\} \qquad q = 0 \qquad (6)$$

MFDFA changes into the conventional DFA when $q = 2$. The meaning of this function is the effect of different degrees of fluctuation on $F_q(s)$ can be described by different q values. When $q < 0$, the larger fluctuation deviation tends to 0 after q power, and it hardly works in the summation. The value of $F_q(s)$ mainly depends on the smaller $F^2(v, s)$. Similarly, when $q > 0$, the larger $F^2(v, s)$ plays a decisive role in the value of $F_q(s)$.

6. The scaling property of fluctuation function can be obtained by analyzing the double logarithmic function of $F_q(s)$

and s. The description of scaling behavior and long-range correlation of $F_q(s)$ by q is embodied in $h(q)$. The $F_q(s)$ has an increasing trend along with s which has a power-law when the time series has the long-range correlation:

$$F_q(s) \sim s^{h(q)} \qquad (7)$$

where $h(q)$ can be called the generalized Hurst exponents. Specially, when $q = 2$, $h(2)$ is transformed into the Hurst exponent $H(q)$. The sequence is a monofractal sequence when $h(q)$ is a constant; that means the scale of mean square error $F^2(v, s)$ shows no difference in all intervals. Conversely, if there is a non-linear relationship between $h(q)$ and q, the series is multifractal series.
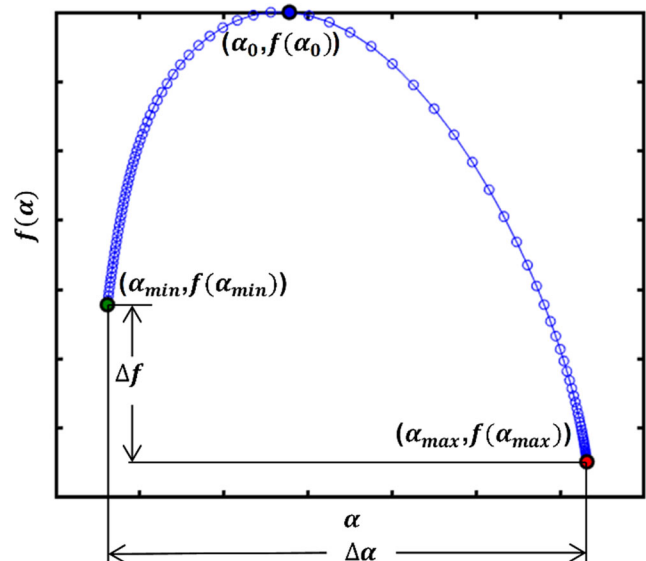

Fig. 3 Schematic diagram of MFDFA features

Table 2 Milling parameters

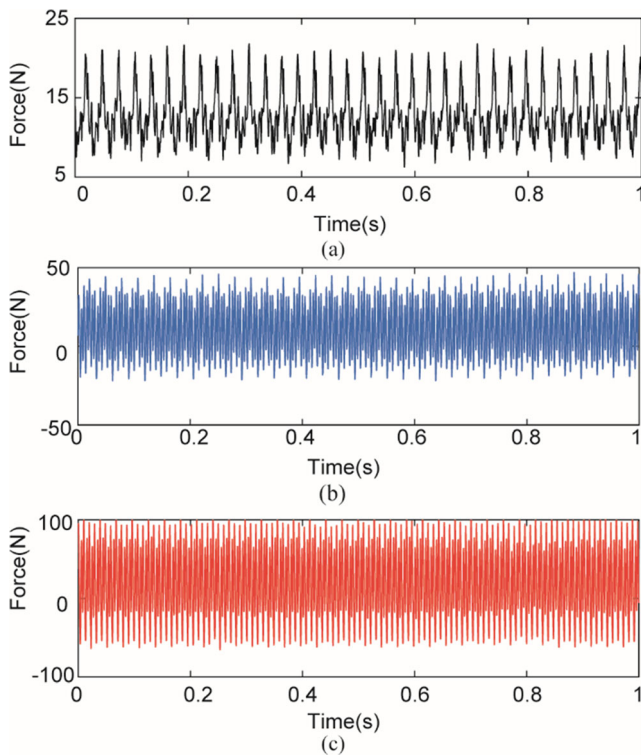| Spindle speed	10,400 rpm
Feed rate	1555 mm/min
Y cut depth (radial)	0.125 mm
Z cut depth (axial)	0.2 mm
Sampling data	50 KHz

Fig. 4 The waveforms of cutting force signal F_x under different tool conditions. (a) The initial wear stage. (b) The gradual wear stage, (c) The accelerated wear stage
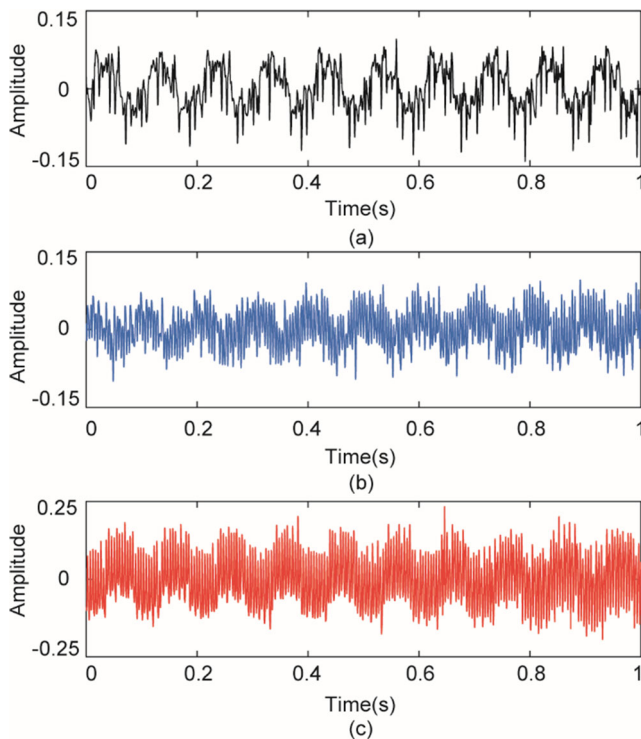

Fig. 5 The waveforms of vibration signal V_x under different tool conditions. (a) The initial wear stage. (b) The gradual wear stage. (c) The accelerated wear stage

7. The relationship between the generalized Hurst exponent $h(q)$ and the mass index $\tau(q)$ in classical multifractal theory is as follows:

$$\tau(q) = qh(q)-1 \qquad (8)$$

The singularity exponent α and the multifractal singularity spectrum $f(\alpha)$ can be obtained by the Legendre transform:

$$\begin{aligned} \alpha &= \tau'(q) = h(q) + qh'(q) \\ f(\alpha) &= q\alpha - \tau(q) \end{aligned} \qquad (9)$$

The parameters of multifractal spectrum can describe the dynamic characteristics of time series. It is an effective tool to analyze non-stationary time series. Tool wear can change the multi-fractal spectrum of cutting signals. Seven multifractal spectrum parameters are employed as MFDFA feature in this paper, which are shown in Fig. 3. Singular exponential α (the abscissa) reflects the unevenness of time series in local probability measure distribution. $f(\alpha)$ (the ordinate) is the fractal dimension which reveals the singular exponents α of distribution. The left point $(\alpha_{min}, f(\alpha_{min}))$ whose slope approaches to positive infinity stands for the maximum fluctuation singularity exponent and its fractal dimension, respectively. In contrast, the right point $(\alpha_{max}, f(\alpha_{max}))$ which has negative infinity slope embodies the minimum fluctuation singularity exponent and its fractal dimension severally. The abscissa of the maximum point of the curve α_0 manifests the randomness of the signal. A larger α_0 means that the signal is more irregular and random. The non-uniformity of probability measure distribution and the proportion of large and small peaks of signals are demonstrated by $\Delta\alpha$ ($\Delta\alpha = \alpha_{max} - \alpha_{min}$) and $\Delta f(\alpha)$ ($\Delta f(\alpha) = f(\alpha_{max}) - f(\alpha_{min})$), respectively. As a result of its clear physical meaning and excellent performance in non-stationary domain, the multifractal parameters can be utilized to analyze intrinsic characteristics of cutting signals.

3.2 Support vector machine

SVM is a classification learning method based on statistical theory. Its basic principle is to construct the optimal classification surface which has the maximal interval by mapping feature space from low dimension to high dimension [38]. The SVM aims to obtain the maximum boundary hyperplane between two classes, which is determined by data points called support vectors, so as to classify test data sets correctly. When solving the non-linear classification problem, the kernel function is applied for non-linear transformation. The data samples in low dimension space are converted to high-dimension space so that the samples can be linearly separable in high-dimension space. The plane for classification is called the optimal classification hyperplane. Introducing the kernel

Fig. 6 The q-order local fluctuation of the initial wear stage cutting force signals. (a) Waveforms of signal F_x. (b) The q-order of the local fluctuations for signal F_x
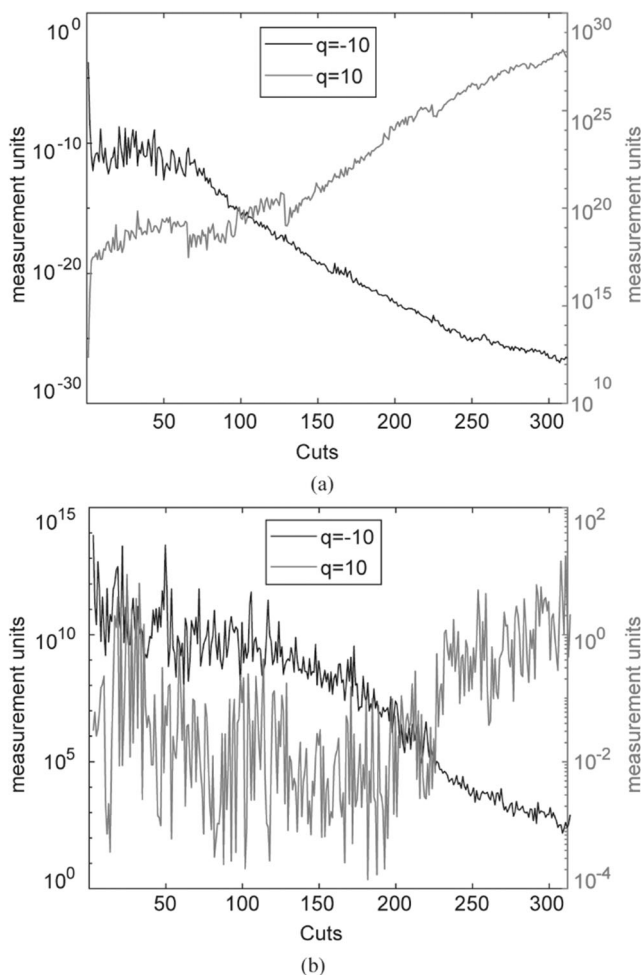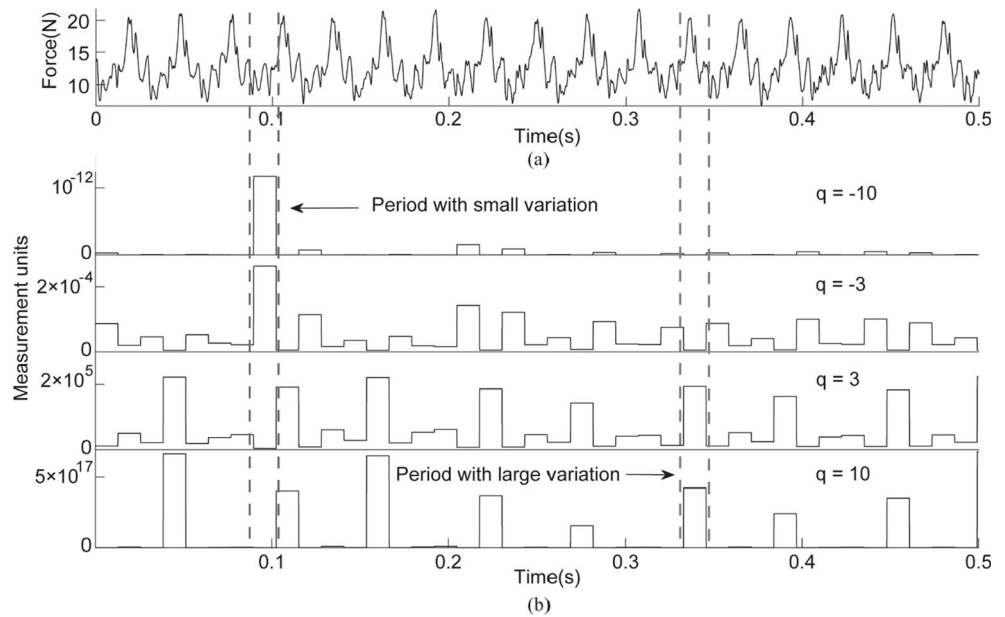
function K instead of the dot product operation solves the computational complexity problem caused by the rising dimension. With a set of training sample $D = \{(x_i, y_i) | i = 1, 2, ..., n\}$, $x_i \in R^n$, the optimal classification hyperplane can be defined as:

$$\langle w, \Phi(x) \rangle + b = 0 \tag{10}$$

where b is intercept and w is the normal vector of the plane. The original problem of solving the optimal classification surface can be simplified to solving the dual problem as below:

$$\begin{cases} \max J(\alpha) = \max\left\{ \sum_{i=1}^{n} \alpha_i - \frac{1}{2} \sum_{i=1}^{n} \sum_{j=1}^{n} \alpha_i \alpha_j y_i y_j K(x_i, x_j) \right\} \\ s.t. \sum_{i=1}^{n} y_i \alpha_i = 0, 0 \leq \alpha_i \leq C, i = 1, 2, \ldots n \end{cases} \tag{11}$$

where $K(x_i, x_j) = \langle \Phi(x_i), \Phi(x_j) \rangle$ is the kernel function, α_i is the Lagrange multiplier, and C is a penalizing factor. The optimal classification function $f(x)$ is obtained as below by solving the quadratic problem:

$$f(x) = \text{sgn}\left[\sum_{i=1}^{n} \alpha_i^* y_i K(x_i, x) + b^* \right] \tag{12}$$

The radial basis function was specified as the kernel function. The kernel function is represented as follows:
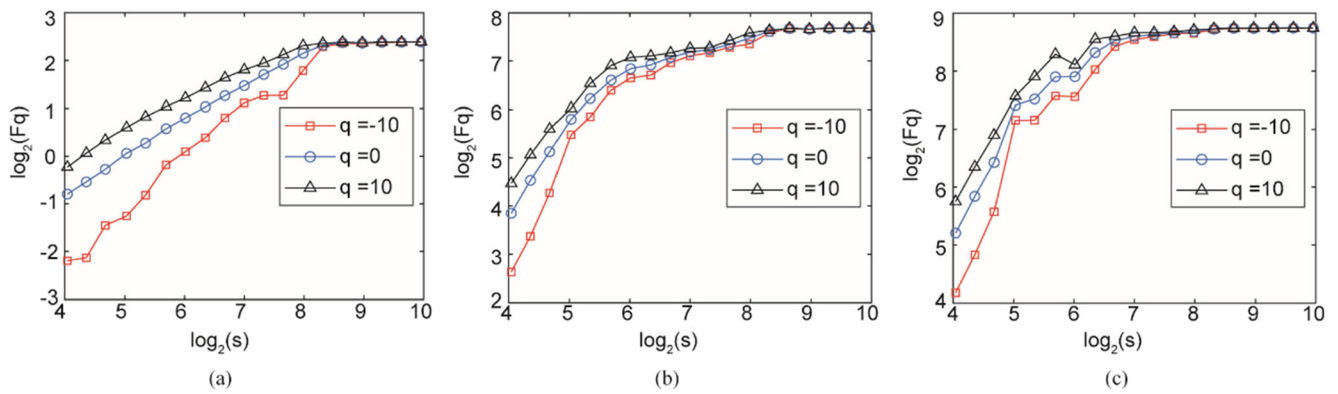
Fig. 7 Variation of maximal q-order local fluctuation value by $q = -10$ and $q = 10$ with cuts. (a) Signal F_x. (b) Signal V_x

Fig. 8 Relationship between the mean square error function $F_q(s)$ and scale s under different wear stages of signal F_x. (a) The initial wear stage. (b) The gradual wear stage. (c) The accelerated wear stage

$$K(x_i, x) = \exp\left(-\gamma \|x - x_i\|^2\right), \gamma > 0 \quad (13)$$

4 Tool condition monitoring based on MFDFA and SVM

In this study, we choose the cutting force and vibration signals to analyze. We select the data collected at the last second of the cutting process in each sample for analysis, which has a more direct relationship with the measured value of tool wear. Figures 4 and 5 show the original cutting force signal F_x and vibration signal V_x under different tool conditions. With the increase of tool wear, the amplitude of cutting force and vibration increases gradually and the waveform becomes more and more intensive. The periodicity of milling force and vibration is gradually drowned. This is mainly due to the fact that the small chatter caused by the increasing tool wear affects the original cutting force and vibration signals. The figure shows that we can only get qualitative change trend rather than quantitative information given from the time-domain

signal. Consequently, it is very difficult to clearly distinguish the three states of the tool wear.

Because milling signal has periodicity, milling signal has periodicity and large fluctuation from the point of view of signal waveform. At the same time, there is small fluctuation between adjacent cycles. Therefore, the variability of fluctuation is also the essential attribute of milling signal. From this point of view, we can study the change of this property in the signals of milling process with the increasing of tool wear. Figure 6 shows the q-order local fluctuation of the initial wear stage cutting force signals. The q-order local fluctuation is described by $[F^2(v, s)]^{q/2}$ computed in Eq. (6), which the scale is 128. The positive q value ($q = 3, 10$) shows the signal is dominated by the large root mean square segments; on the contrary, the negative q value ($q = -3, -10$) shows the signal is controlled by the small root mean square segments. The signal has more obvious property of small or large fluctuation when the q has larger absolute value. From Fig. 6, we can see that the abrupt segment of milling force signal has a large q-order fluctuation value when q is positive and the sequences between the two peaks have large q-order fluctuation value when q is negative. Therefore, the q-order local fluctuation value can clearly distinguish the large and small fluctuation
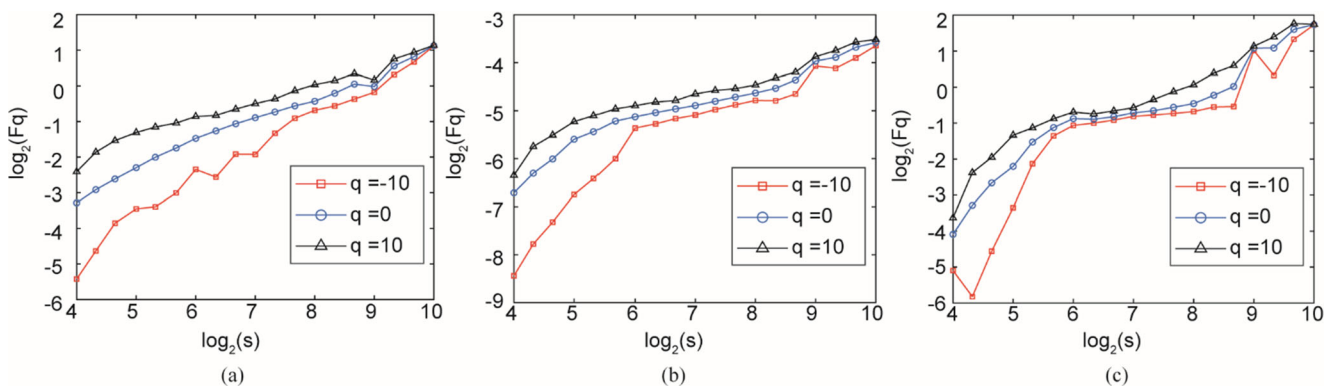

Fig. 9 Relationship between the mean square error function $F_q(s)$ and scale s under different wear stages of signal V_x. (a) The initial wear stage. (b) The gradual wear stage. (c) The accelerated wear stage
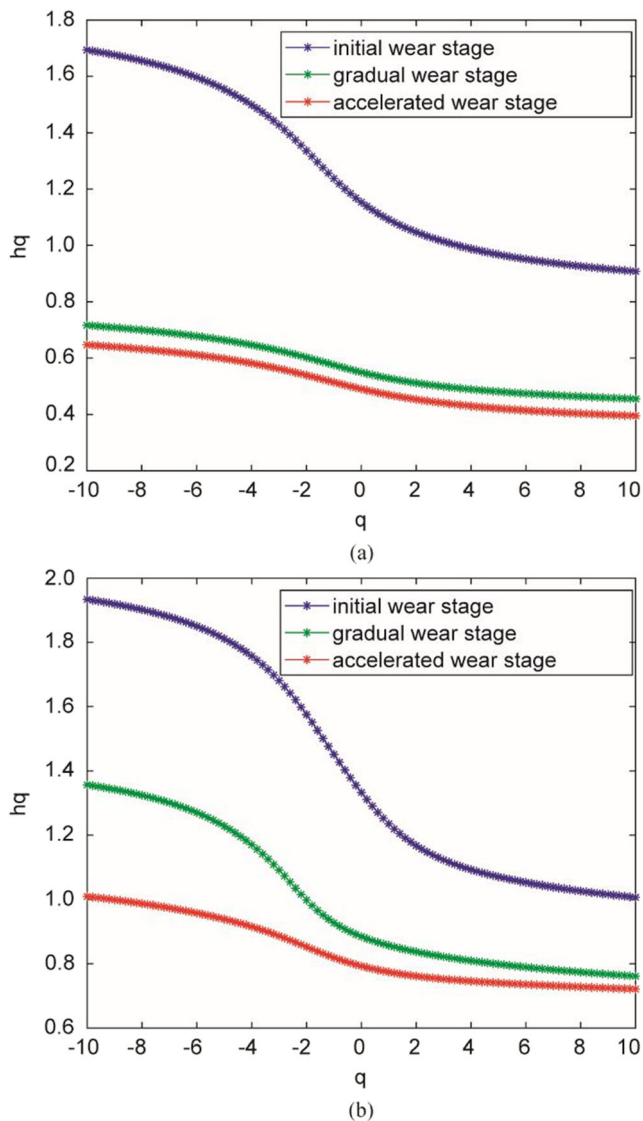
Fig. 10 Relationship between the generalized Hurst exponents $h(q)$ and q under different wear stages. (a) Signal of F_x. (b) Signal of V_x

parts of milling signal and the large q-order fluctuation value of positive and negative q appears alternately and periodically. Figure 7 shows the variation of maximal large and small fluctuation value in the tool wear life. When q is positive ($q = 10$), q-order local fluctuation value increases with the increase of cutting times. In contrast, when q is negative ($q = -10$), the values decrease with the increase of cutting times. This means that the large fluctuation becomes more and more obvious in the process of tool wear and the small fluctuation decreases gradually in this process. Therefore, it can be seen that there is a positive or negative correlation between signal fluctuation amplitude and tool wear. Multifractal method is one of the effective methods to study the change of fluctuation amplitude.

Relation between the mean square error function $F_q(s)$ and scale s under different wear stages of F_x and V_x is shown in

Fig. 8 and Fig. 9. The figure shows that the logarithmic curves of $F_q(s)$ and s of cutting force signal and vibration signal have a certain linear relationship. That means $F_q(s)$ and s well satisfy the power law relationship under different conditions of cutting tools. In addition, the power law relationship is stronger with the increasing tool wear. The results show that the tool wear force and vibration signals at different wear stages have scaling invariance and multifractal characteristics on a certain scale.

Relationship between the generalized Hurst exponents $h(q)$ and q under different wear stages is shown in Fig. 10. It can be seen that the Hurst exponent $h(q)$ of cutting force signals and vibration signals both varies non-linearly with the q value in different cutting tool states, which indicates that both the cutting tool signals and vibration signals are multifractal sequences. Besides, from this figure, we can obtain that when the tool changes from the initial wear stage to the accelerated wear stage, the generalized Hurst exponent of both cutting force signal and vibration signal shows a decrease. We notice that the Hurst exponent of cutting force signals under the initial wear and the gradual wear condition and vibration signals in the whole tool wear life is greater than 0.5, which indicates that there is a long-range correlation in the initial wear state because the signals basically only have the fundamental frequency signal in this condition. In contrast, the Hurst exponent of cutting force signals under the accelerated wear state is less than 0.5, which indicates that the signals in this condition are negative long-range correlation. Because the signal in the sharp wear state contains both the impact noise signals and the cutting fundamental frequency signals, the impact signal is more prominent.

The multifractal spectrum is shown in Fig. 11. The figure shows that the shape of multifractal spectrum is single peak and the maximum value is 1, which fully shows that the cutting signal has multifractal characteristics. Moreover, from Fig. 11, it can be seen that the range of multifractal spectrums in different states is obviously different, but the multifractal spectrums in Fig. 11(e) cluster close together and cannot be distinguished. Besides, from the perspective of ordinates, in Fig. 11 (a) and (b), $f(\alpha)$ of the left point and the right point in multifractal curves decreases with the increase of tool wear. However, in Fig. 11(c) and (d) $f(\alpha)$ of these point loses the monotonic decrement, which means the $f(\alpha)$ eigenvalues extracted from these multifractal spectrums will judge some tool states incorrectly. In this work, the α_{max}, α_{min}, α_0, $\Delta\alpha$, $f(\alpha_{max})$, $f(\alpha_{min})$, Δf of multifractal spectrums are calculated as feature parameters which can reflect the tool wear state. Seven features are extracted from three-dimensional force signal (F_x, F_y, F_z) and vibration signal(V_x, V_y, V_z), respectively, to form a 42-dimensional feature matrix for pattern recognition.

Multi-fractal feature parameters extracted from different wear stages are used as input parameters. Ninety groups of data were extracted in every experiment, including 30 groups
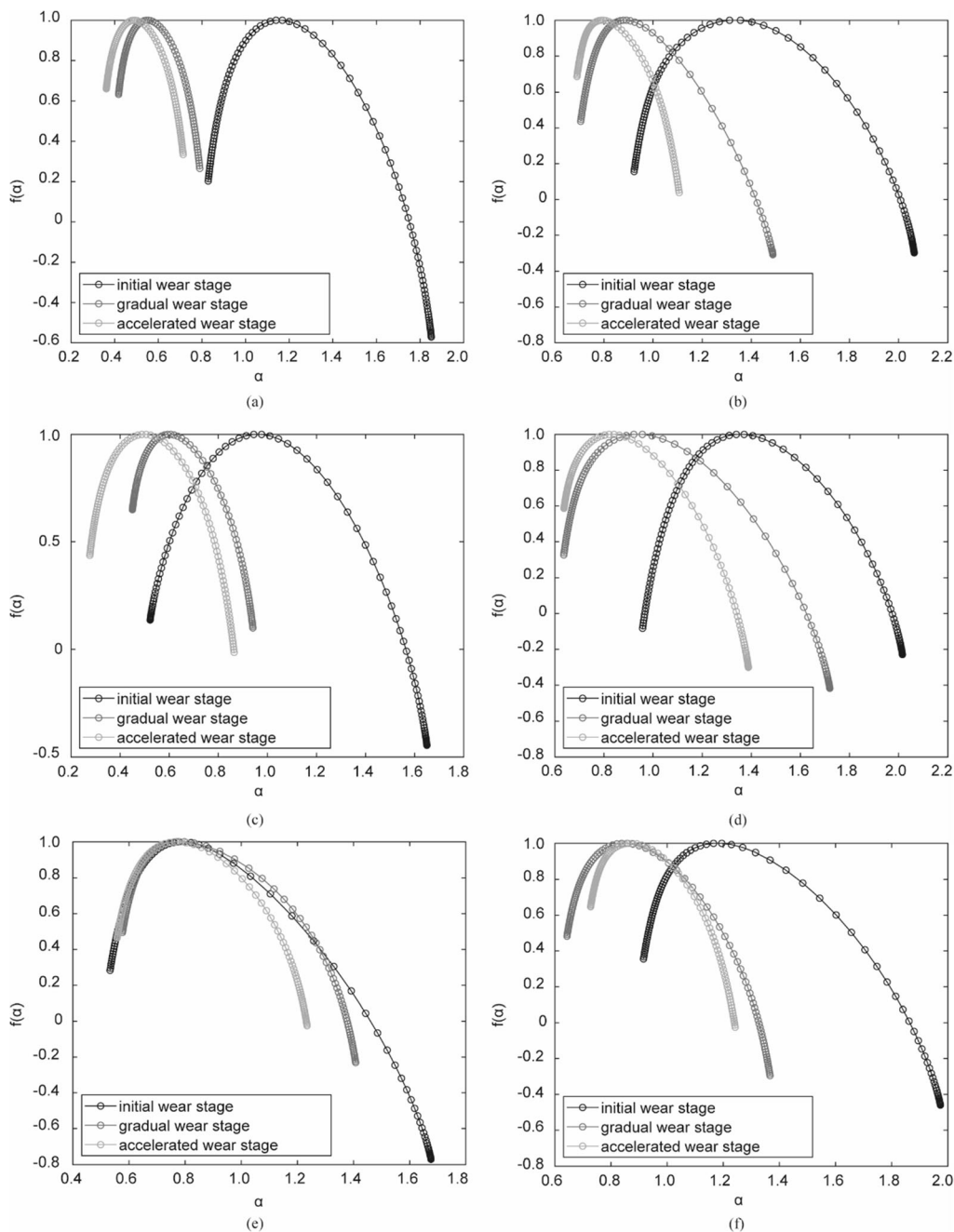
Fig. 11 Multifractal spectrum of under different wear stages. (a) Signal of F_x. (b) Signal of V_x. (c) Signal of F_y. (d) Signal of V_y. (e) Signal of F_z. (f) Signal of V_Z

of data for each condition of tool wear. Therefore, 270 groups of data were extracted. They were divided into two groups: The first group includes 180 samples, which were used for train SVM model. The other groups including 90 samples are the test set. Before building the SVM model, the feature matrix should have a zero-mean normalization processing which is helpful for improvement of train speed and accuracy. Then, the SVM model for tool condition monitoring will be trained by using training samples and the corresponding labels. The kernel function of SVM adopts radial basis function,

because the Gaussian kernel can make the sample space map from low-dimension to higher dimensional space, so that the model can get better classification effect. Previous studies have shown that the SVM model trained by radial basis function has better performance in small sample data, which is consistent with the cutting process, because the data collected from cutting experiments are limited and the amount of data is much smaller than that in other fields such as big data analysis. The important argument cost c and gamma g will be determined by grid-search with cross-validation method. The

parameter c represents the penalty coefficient, and the parameter g comes from the radial basis function which is related to the variance. The parameters of c and g are selected by meshing method, traversing the two parameters from -5 to 5 in double logarithmic coordinates. Each group of parameters is trained by SVM. At the same time, cross-validation method is used, that is, the training set is divided into equal parts, one test set is selected each time, the other is training set, and the c and g with the highest recognition rate are selected as the parameters of SVM type that is used to identify test set data. In this study, the best g and c are obtained as 4 and 32, respectively, and the tool wear model is well constructed.

Finally, test data are utilized to verify model prediction accuracy. The prediction results and the actual state are presented in Fig. 12. The result shows that the accuracy of this model is 95.6%. As shown in Table 3, the accuracy results obtained in this paper are higher than those of published research in recent years. There are various data sources in fault diagnosis and condition monitoring for different machining methods (such as turning, milling, grinding) is different, cutting parameters (such as cutting speed, feed, and cutting depth) are different, and acquisition signals (such as cutting force signal, vibration signal, and acoustic emission signal) are different. All of these above conditions will cause different data sets, which is related to the specific research field and experimental design method of researchers. It is rare to use the same data to study the same problem. Even if the same data is used, due to different handing methods, the selection of various parameters in the training model will be greatly different. The change of one condition often leads to the change of the whole model, and only one factor is changed. It is difficult to realize the comparison of other invariant control variable methods in the field of fault diagnosis. So the result fully reflects that the method of MFDFA combined with SVM can more accurately identify the different states of tool wear, and shows its advantages in the field of tool wear monitoring.
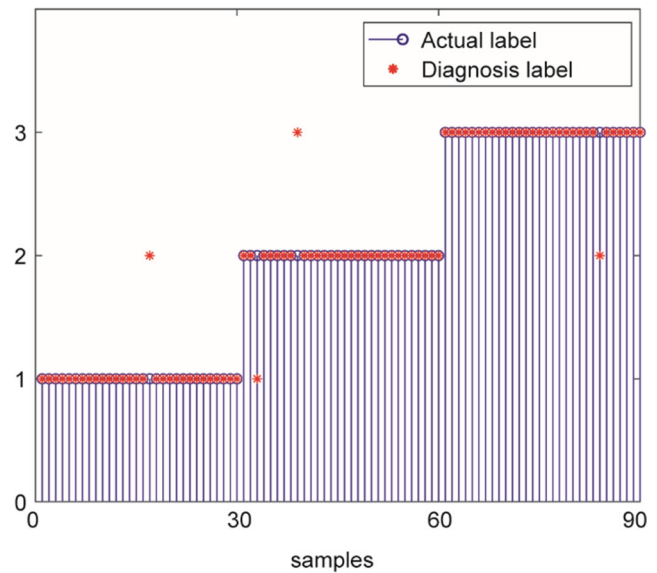

Fig. 12 Classification result of tool wear condition based SVM model ((1) the initial wear stage, (2) the gradual wear stage, (3) the accelerated wear stage)

Compared with [34, 39], this method has a higher accuracy when SVM is also used as the classification model. It shows that the features extracted by MFDFA are more sensitive to tool wear than the features in time domain and frequency domain. And it is more targeted and applicable to analyze the trend of signal fluctuation amplitude during tool wear processing from the inherent characteristics of the cutting process and then use the MFDFA method to calculate and characterize this trend. Moreover, the accuracy of this method is still higher than [39] without feature selection, which has obvious advantages and great significance in reducing calculation amount and improving calculation speed.

It should be noted that other methods in the comparative literature [34, 39–43] mostly use time domain features (mean, root mean square, standard deviation, skewness, kurtosis,

Table 3 Comparison with published results of tool condition monitoring	Refs.	Extracted features	Classification model	Accuracy rate
	Hu et al. [39]	Time domain, frequency domain	ν-Support vector machine	62% (before feature selection)
				84.3% (after feature selection)
	Kothuru et al. [34]	Frequency domain	SVM	95%
	Hong et al. [40]	Wavelet transform	Hidden Markov models	86.7%
	Cao et al. [41]	Frequency domain	Convolutional neural network	92.2%
	Rizal, M., et al. [42]	Time domain, frequency domain	Mahalanobis-Taguchi system	88.89%
	Xie et al. [43]	Time domain, wavelet transform	Continuous hidden Markov models	90%
	This paper with the proposed method	Multifractal features	SVM	95.6%

etc.), frequency domain features (mean square frequency, frequency variance, frequency band energy, etc.), and time-frequency domain (wavelet transform and other parameters). The validity of these parameters is widely confirmed and can establish a good correlation with tool wear. However, because these parameters are statistical characteristic parameters, they focus on the change of sample data statistics, thus ignoring the source and inherent properties of sample data itself. These data samples come from the cutting process, which is the direct contact and relative movement between the tool and the workpiece material. With the gradual wear of the tool, the change of this movement is reflected in the signal sample. With regard to the MFDFA method in this paper, the signal fluctuates greatly and violently all the time based on the periodic characteristics of milling. It is found that with the increase of tool wear, the large amplitude fluctuation of the signal becomes larger and larger, and the small-amplitude fluctuation decreases gradually (as shown in Fig. 6 and Fig. 7). The extracted multifractal characteristic parameters have clear physical meanings. The change of cutting process signal is explained from the point of view of fractal behavior, not just the change of mathematical statistics without clear physical meaning. This is the advantage of MFDFA compared with other methods in the literature.

For the scope of application of current research results, there exist the differences of machining methods, workpiece materials, and cutting parameters. For the same machining methods and different cutting parameters, the tool wear measurements and signal acquisitions under all the cutting parameters and their combinations cannot be achieved in the experiments, so it is only investigated under the fixed cutting parameters. In this paper, the variations of cutting signal magnitude and amplitude are studied, and the relevant features are extracted by the MFDFA method for analysis. Under the conditions of different cutting parameters in the cutting process, the complete tool life process is in the same variation with large fluctuation increasing and small fluctuation decreasing, so it can be applied to different cutting parameters. For different machining methods, due to the change of material removal mechanism, the machining motions of turning, milling, and grinding are different, and the inherent signal difference is huge. The application of this method in other machining methods needs to be investigated in depth in the future.

5 Conclusions

This paper proposes a method of MFDFA and SVM for tool condition monitoring. Firstly, combined with the inherent mechanism of milling and the performance characteristics of milling signals, it is found that in the process of milling, with the aggravation of tool wear, the large amplitude fluctuations of signals gradually increase, while the small-amplitude

fluctuations gradually decrease. Since multifractal spectrum parameters can represent signal fluctuation, the MFDFA is employed to analyze the non-stationary property and extract the feature from cutting force signals and vibration signals. Results show that the tool wear signal has long-range correlation and obvious multi-fractal characteristics. In addition, different wear stages of the tool can be clearly distinguished by the multi-fractal spectrum parameters, which indicates the multi-fractal spectrum parameters are sensitive to the tool wear. Secondly, fault detection is carried out by SVM with input of eigenvectors constituted by the multifractal feature parameters. The result shows that the proposed methods of MFDFA and SVM can identify the different tool wear stages well and the accuracy reaches up to 95.6%. In the future work, the modified approach of the above-presented method or other new method for signal preprocessing and feature dimension reduction is in progress to achieve higher accuracy.

References

1. Nouri M, Fussell BK, Ziniti BL, Linder E (2015) Real-time tool wear monitoring in milling using a cutting condition independent method. Int J Mach Tools Manuf 89:1–13
2. Javed K, Gouriveau R, Li X, Zerhouni N (2018) Tool wear monitoring and prognostics challenges: a comparison of connectionist methods toward an adaptive ensemble model. J Intell Manuf 29(8): 1873–1890
3. Zhou Y, Xue W (2018) A multisensor fusion method for tool condition monitoring in milling. Sensors 18(11):3866
4. Jemielniak K, Kosmol J (1995) Tool and process monitoring-state of art and future prospects. Scientific papers of the institute of mechanical engineering and automation of the Technical University of Wroclaw 61:90–112
5. Oguamanam DC, Raafat HM, Taboun SM (1994) A machine vision system for wear monitoring and breakage detection of single-point cutting tools. Comput Ind Eng 26(3):575–598
6. Yesin T, Ozel Z (1986) A study of cutting tool wear by neutron activation technique. J Radioanal Nucl Chem 99(2):441–445
7. Cook NH (1980) Tool Wear Sensors. Wear 62(1):49–57
8. Pratama M, Dimla E, Lai CY, Lughofer E (2019) Metacognitive learning approach for online tool condition monitoring. J Intell Manuf 30(4):1717–1737
9. Gao D, Liao Z, Lv Z, Lu Y (2015) Multi-scale statistical signal processing of cutting force in cutting tool condition monitoring. Int J Adv Manuf Technol 80(9-12):1843–1853
10. Freyer BH, Heyns PS, Theron NJ (2014) Comparing orthogonal force and unidirectional strain component processing for tool condition monitoring. J Intell Manuf 25(3):473–487
11. Antic A, Simunovic G, Saric T, Milosevic M, Ficko M (2013) A model of tool wear monitoring system for turning. Teh Vjesn 20(2): 247–254

12. Hsieh W, Lu M, Chiou S (2012) Application of backpropagation neural network for spindle vibration-based tool wear monitoring in micro-milling. Int J Adv Manuf Technol 61(1):53–61

13. Kannateyasibu E, Yum J, Kim TH (2017) Monitoring tool wear using classifier fusion. Mech Syst Signal Process 85:651–661

14. Kosaraju S, Anne VG, Popuri BB (2013) Online tool condition monitoring in turning titanium (grade 5) using acoustic emission: modeling. Int J Adv Manuf Technol 67(5-8):1947–1954

15. Singh D, Rao PV (2010) Flank wear prediction of ceramic tools in hard turning. Int J Adv Manuf Technol 50(5-8):479–493

16. Lin XK, Zhou B, Zhu L (2017) Sequential spindle current-based tool condition monitoring with support vector classifier for milling process. Int J Adv Manuf Technol 92(9-12):3319–3328

17. Arslan H, Er AO, Orhan S, Aslan E (2016) Tool condition monitoring in turning using statistical parameters of vibration signal. Int J Acoust Vib 21(4):371–378

18. Bhuiyan MS, Choudhury IA, Dahari M, Nukman Y, Dawal SZ (2016) Application of acoustic emission sensor to investigate the frequency of tool wear and plastic deformation in tool condition monitoring. Measurement 92:208–217

19. Wu Y, Escande P, Du R (2001) A new method for real-time tool condition monitoring in transfer machining stations. J Manuf Sci Eng Trans ASME 123(2):339–347

20. Gong WG, Obikawa T, Shirakashi T (1997) Monitoring of tool wear states in turning based on wavelet analysis. JSME Int J Ser C-Mech Syst Mach Elem Manuf 40(3):447–453

21. Babouri MK, Ouelaa N, Djebala A (2016) Experimental study of tool life transition and wear monitoring in turning operation using a hybrid method based on wavelet multi-resolution analysis and empirical mode decomposition. Int J Adv Manuf Technol 82(9):2017–2028

22. Zhu KP, Wong YS, Hong GS (2009) Wavelet analysis of sensor signals for tool condition monitoring: a review and some new results. Int J Mach Tools Manuf 49(7):537–553

23. Kantelhardt JW, Zschiegner S, Koscielnybunde E, Havlin S, Bunde A, Stanley HE (2002) Multifractal detrended fluctuation analysis of nonstationary time series. Phys A Stat Mech Appl 316(1-4):87–114

24. Xiong Q, Zhang W, Lu T, Mei G, Liang S (2016) A fault diagnosis method for rolling bearings based on feature fusion of multifractal detrended fluctuation analysis and alpha stable distribution. Shock Vib 2016:1232893

25. Liu H, Jing J, Ma J (2018) Fault diagnosis of electromechanical actuator based on VMD multifractal detrended fluctuation analysis and PNN. Complexity 2018:9154682

26. Pal S, Heyns PS, Freyer BH, Theron NJ, Pal SK (2011) Tool wear monitoring and selection of optimum cutting conditions with progressive tool wear effect and input uncertainties. J Intell Manuf 22(4):491–504

27. Cho SY, Binsaeid S, Asfour S (2010) Design of multisensor fusion-based tool condition monitoring system in end milling. Int J Adv Manuf Technol 46(5-8):681–694

28. Geramifard O, Xu J, Zhou J, Li X (2012) A physically segmented hidden Markov model approach for continuous tool condition monitoring: diagnostics and prognostics. IEEE Trans Ind Inf 8(4):964–973

29. Lu MC, Wan BS (2013) Study of high-frequency sound signals for tool wear monitoring in micromilling. Int J Adv Manuf Technol 66(9-12):1785–1792

30. Li N, Chen Y, Kong D, Tan S (2017) Force-based tool condition monitoring for turning process using v -support vector regression. Int J Adv Manuf Technol 91(1):351–361

31. Zhang K, Yuan H, Nie P (2015) A method for tool condition monitoring based on sensor fusion. J Intell Manuf 26(5):1011–1026

32. Gajate A, Haber RE, Toro RM, Vega P, Bustillo A (2012) Tool wear monitoring using neuro-fuzzy techniques: a comparative study in a turning process. J Intell Manuf 23(3):869–882

33. Azmi AI (2015) Monitoring of tool wear using measured machining forces and neuro-fuzzy modelling approaches during machining of GFRP composites. Adv Eng Softw 82:53–64

34. Kothuru A, Nooka SP, Liu R (2018) Application of audible sound signals for tool wear monitoring using machine learning techniques in end milling. Int J Adv Manuf Technol 95(9-12):3797–3808

35. Pandiyan V, Caesarendra W, Tjahjowidodo T, Tan HH (2018) In-process tool condition monitoring in compliant abrasive belt grinding process using support vector machine and genetic algorithm. J Manuf Process 31:199–213

36. PHM Society (2010) PHM Data Challenge, https://www.Phmsociety.org/competition/phm/10S

37. Lu X, Zhao H, Lin H, Wu Q (2016) Multifractal analysis for soft fault feature extraction of nonlinear analog circuits. Math Probl Eng 2016:7305702

38. Cristianini N, Taylor JS (2000) An introduction to support vector machines and other kernel-based learning methods. Cambridge University Press

39. Hu M, Ming W, An Q, Chen M (2019) Tool wear monitoring in milling of titanium alloy Ti–6Al–4 V under MQL conditions based on a new tool wear categorization method. Int J Adv Manuf Technol 104(9):4117–4128

40. Hong Y, Yoon H, Moon J, Cho Y, Ahn S (2016) Tool-wear monitoring during micro-end milling using wavelet packet transform and Fisher's linear discriminant. Int J Precis Eng Manuf 17(7):845–855

41. Cao X, Chen B, Yao B, Zhang S (2019) An intelligent milling tool wear monitoring methodology based on convolutional neural network with derived wavelet frames coefficient. Appl Sci 9(18):3912

42. Rizal M, Ghani JA, Nuawi MZ, Haron CHC (2017) Cutting tool wear classification and detection using multi-sensor signals and Mahalanobis-Taguchi System. Wear 376-377:1759–1765

43. Xie Z, Li J, Lu Y (2019) Feature selection and a method to improve the performance of tool condition monitoring. Int J Adv Manuf Technol 100(9):3197–3206